Polish Journal of Veterinary Sciences Vol. 20, No. 2 (2017), 395–402

DOI 10.1515/pjvs-2017-0048

Original article

Horizontal transfer and functional evaluation of high pathogenicity islands in Avian *Escherichia coli*

J. Tu, K. Qi, X. Song, T. Xue, H. Ji, Y. Shao, H. Liu, X. Zhou, L. Zhu

College of Animal Science and Technology, Anhui Agriculture University, Hefei, Anhui 230036, China
Anhui Province Key Laboratory of Veterinary Pathobiology and Disease Control, Hefei, Anhui 230036, China

Abstract

High pathogenicity islands (*HPI*s) in *Escherichia coli* encode genes that are primarily involved in iron uptake and regulation, and confer virulence and pathogenicity. The aim of this study was to investigate the transfer of *HPI*s in avian *E. coli* and identify the function of *HPI* in the acceptor strain. The *HPI* transfer strain was obtained under conditions of low temperature and low iron abundance, and the donor and acceptor strains were confirmed. *E. coli HPI*s are transferred by horizontal gene transfer events, which are likely mediated primarily by homologous recombination in *HPI*-adjacent sequences. Assays for biological activity and pathogenicity changes in the acceptor strain indicated that *HPI*s might not be involved in pathogenesis in avian *E. coli*, and thus the main function of *HPI*s in this strain of bacteria may be to regulate iron nutrition.

Key words: Avian *Escherichia coli*, high pathogenicity island, horizontal transfer, iron uptake function, pathogenicity

Introduction

Pathogenicity islands code for toxins, adhesins, invasins, or other virulence factors, and may be transmitted via transposons, plasmids, or bacteriophages (Hacker et al. 1997). In addition, such genes may be part of particular regions on the bacterial chromosome termed high pathogenicity islands (*HPIs*). For example, the *HPI* in the *Yersinia* bacteria chromosome is a region of clustered genes that plays a key role in *Yersinia* toxicity in mice and is closely associated with lethality (Pulludat et al. 1998). The *Yersinia HPI* mainly includes virulence genes that are associated with iron uptake, including yersiniabactin (*Ybt*, a siderophore) and its regulatory genes, which function in iron uptake (Heesemann et al. 1993). Furthermore, the *Yersinia HPI* is located adjacent to a tRNA gene (Asn-tRNA) (Heesemann et al. 1993, Rakin et al. 1999). Avian pathogenic *Escherichia coli* (APEC) infection is responsible for morbidity and mortality in poultry that lead to significant economic losses in the poultry industry worldwide (Fairbrother JM et al. 1999, Kaper JB et al. 2004). Avian *E. coli* is a significant pathogenic bacteria species that causes avian colibacillosis in poultry worldwide. The main clinical manifestations of avian colibacillosis are airsacculitis, perihepatitis, pericarditis and encephalitis. More specifically, several studies have shown that the

Correspondence to: K. Qi, e-mail: qkz@ahau.edu.cn

Table 1. Primers used in this study.

Primers	Oligonucleotide sequence (5' to 3')	Product size (bp)
irp2-F irp2-R	AAGGATTCGCTGTTACCGGAC AACTCCTGATACAGGTGGC	414
intB-F intB-R	GAACGGCGGACTGTTAAT ATCGCTTTGCGGGCTTCTAGG	1337 or 990
ERIC-1 ERIC-2	ATGTAAGCTCCTGGGGATTCAC AAGTAAGTGACTGGGGTGAGCG	–

HPI core region of *E. coli* is nearly identical to that of *Yersinia* bacteria, and revealed the highly conserved features of *HPIs* across bacteria species. The homology of the *E. coli* and *Yersinia HPI* core region genes *irp1*, *irp2, irp3, irp4*, *irp5*, and *fyuA* is 98%, 98%, 98%, 95%, 98% and 98%, respectively (Xu et al. 2010). The structural features and wide distribution of the *HPI* in intestinal *E. coli* suggest that it is transmitted via horizontal gene transfers, but the horizontal transfer of the *HPI* in avian *E. coli* via co-culture methods at low temperature and in a low iron liquid medium has not been reported.

In this study, we used clinical isolates of avian *E. coli* with co-culture methods in a low iron liquid medium to verify the horizontal transfer of the *E. coli HPI*. Polymerase chain reaction (PCR) was used to assay for *HPI* transfer from the donor to the recipient bacteria. By evaluating biological functions in the *HPI* recipient strain together with its pathogenicity, the impact of *HPI* on pathogenicity and iron uptake in avian *E. coli* was determined.

Materials and Methods

Bacterial strains and culture conditions

The wild-type strain was a clinical isolate of Avian pathogenic *E. Coli* strain AE17 (serotype O2) that was collected from a chicken in Anhui Province, China in 2008. The bacteria used in the experiments reported herein were grown routinely in Lennox broth (LB) and LB with iron deficiency (containing 2,2'-bipyridine), or on 1.5% solid LB medium at 37°C.

Chloramphenicol (34 mg/ml) was added to the medium for the antibiotic group.

Animals

In the experiments, we used the one-day-old Roman hens, which were purchased from Anhui Anqin Poultry Company Ltd. (Anhui Province, China). These hens were euthanized using administered intravenously sodium pentobarbital (100 mg/kg, Dolethal, Vétoquinol, Cedex, France) in the wing vein.

Selection of avian *E. coli* donor and acceptor strains for *HPI* transfer and co-culture

According to the results of *HPI* assays and drug resistance tests in avian *E. coli*, three chloramphenicol-resistant HPI^- isolates were selected as acceptor strains, and were named AE-a1, AE-a2, and AE-a3. Two HPI^+ isolates without chloramphenicol resistance were chosen as donor strains, and were named AE-d1 and AE-d2. The acceptor strains and donor strains were inoculated together and co-cultured in LB containing 1% 2,2'-bipyridine, and co-cultured at 4°C (Lesic and Carniel 2005). Several acceptor or donor strains were selected to increase the possibility on horizontally transfer of HPI between these strains.

Selection of an *HPI*-positive transfer strain and analysis of donor and acceptor strains

The above-mentioned co-cultures were streaked in a flat dish containing chloramphenicol and cultured at 37°C for 12 h. All strains on the flat dish were picked randomly for analysis as the HPI^+ stains by polymerase chain reaction (PCR) assay for the presence of the *irp2* gene (Table 1) (Cheng et al. 2006). The HPI^+ *E. coli* strains as the transfer-positive strains named AE-t. The AE-a1, AE-a2, AE-a3, AE-d1, AE-d2 and AE-t stains were inoculated in 5 mL LB at 37°CC for 12 h and then their bacterial DNA was extracted using a DNA Extraction Kit (SHANGHAI SHENGGONG Bio-engineering Co., Ltd., China). Enterobacterial repetitive intergenic consensus polymerase chain reaction (ERIC- PCR) (Versalovic et al. 1991) was used to analyze the genome homology of these *E. coli* stains. PCR products were separated lay 1% (w/v) agarose gel electrophoresis. For statistical analysis of the amplified products, the positive amplified bands and negative amplified bands were counted as 1 and 0, respectively, and a data matrix was set up for cluster analysis. Genotype differences and correlations between strains were compared in order to identify the *HPI* acceptor strain from among the AE-a1, AE-a2, and

AE-a3 strains. The AE-d1, AE-d2 and AE-t stains were inoculated in LB at 37°C for 12 h, and PCR was used to amplify the *irp2* and *intB* genes. The source of the AE-t *HPI* was determined by comparison with AE-d1 and AE-d2.

Detection of iron uptake capacity by the CAS method

The improved chrome azurol S (CAS) method (Schwyn and Neilands 1987) was used to detect siderophores in the transfer strain, acceptor strain, and donor strain. The AE-a1, AE-t, AE-d2 strains were inoculated in LB at 37°C, and then diluted 1:100 in LB at 37°C for 12 h. Two mL of culture fluid was collected in a 2-mL microcentrifuge tube and centrifuged at 5000 × *g* for 10 min. The supernatant was discarded, the bacteria were resuspended in fresh LB, and absorbance was measured at 600 nm.

The processed bacterial suspensions (10 µL) were inoculated on CAS plates, and 10 µL sterile LB broth served as the treatment for the blank control group. The plates were incubated at 37°C. Changes in the colored area around the colony were assayed every 24 h until no change in colony diameter was observed. The siderophore carrier capacity was calculated based on the radius of the region in which the color changed from blue to orange.

Detection of iron uptake capacity in a low iron environment

First, 200 µL of LB was dispensed into each well of a 96-well plate, and various amounts of 2,2'-bipyridine were added (0.128 mM, 0.256 mM, 0.384 mM, 0.512 mM, 0.640 mM, 0.768 mM, and 0.896 mM). Next, 20 µL AE-a1 or 20 µL AE-t stains were respectively added to liquid medium at the same cells' concentrations. All tests were carried out three times and the results were averaged. Plates were cultured aerobically without shaking at 37 °C, and the absorbance was measured at 600 nm every 12 h.

Assays for bacterial adherence and invasion

Briefly, DF-1 chicken fibroblast cells (DF-1 is an immortalized cell line of chicken embryo fibroblasts) were grown in 24-well cell culture plates to 90% confluence. Cells were infected with 200 multiplicity of infection (MOI) of AE-a1 and AE-t in Dulbecco's Modified Eagle's Medium (DMEM), and incubated at 37°C in 5% CO_2 for 1.5 h. After three washes with PBS to remove nonadherent bacteria, the cells were lysed with 100 mL of 0.5% Triton X-100, and 900 mL of DMEM was added. The resulting cell suspension was serially diluted 10-fold with PBS and spread onto LB agar plates to determine the frequency of adherence. For the invasion assay, cell culture, infection, and bacterial counting were performed as described above for the bacterial adherence assay. The cells were treated subsequently with 100 mg/mL gentamycin at 37°C for 1 h, and lysed with 0.5% Triton X-100. The bacteria were counted and the invasion frequency was determined. All assays for adherence and invasion were performed in three times.

Study of animal infection

Animals were infected with AE-a1 and AE-t to determine the pathogenicity of these strains during systemic infection. Briefly, two groups (n = 10 each) of 7-day-old chicks were intraperitoneally inoculated (IP inoculation) with a bacterial suspension containing 1.6×10^9 CFU/ml. The control group was injected with PBS. Mortality was monitored until 7 days after infection.

Statistical analysis

Data are expressed as mean + standard error of the mean (SEM) from six independent replicates (n=3). Significant differences were analyzed by one-way or two-way analysis of variance (ANOVA) using SAS software version 9.2. Differences with P-values less than 0.05 were considered statistically significant. The direction and degree of each correlation were studied via Pearson's coefficient (±r). The significance of r also was tested at the 5% significance level for the appropriate degrees of freedom using a two-tailed test. Significant differences are marked by *a* ($p<0.05$) or *A* ($p<0.01$).

Results

The identification of the *HPI*-positive transfer strain, acceptor strain, and donor strain

The HPI^+ strains were identified on the fifth day after co-culture by the detection of the *irp2* and *intB* genes via ERIC-PCR (Fig. 1A). The donor strains (AE-d) and the acceptor strains (AE-a) showed the largest difference (more than 15%) in genetic coefficient. The genetic similarity of AE-t and AE-a1 was 100%. As shown in Fig. 1B, a 414-bp PCR product

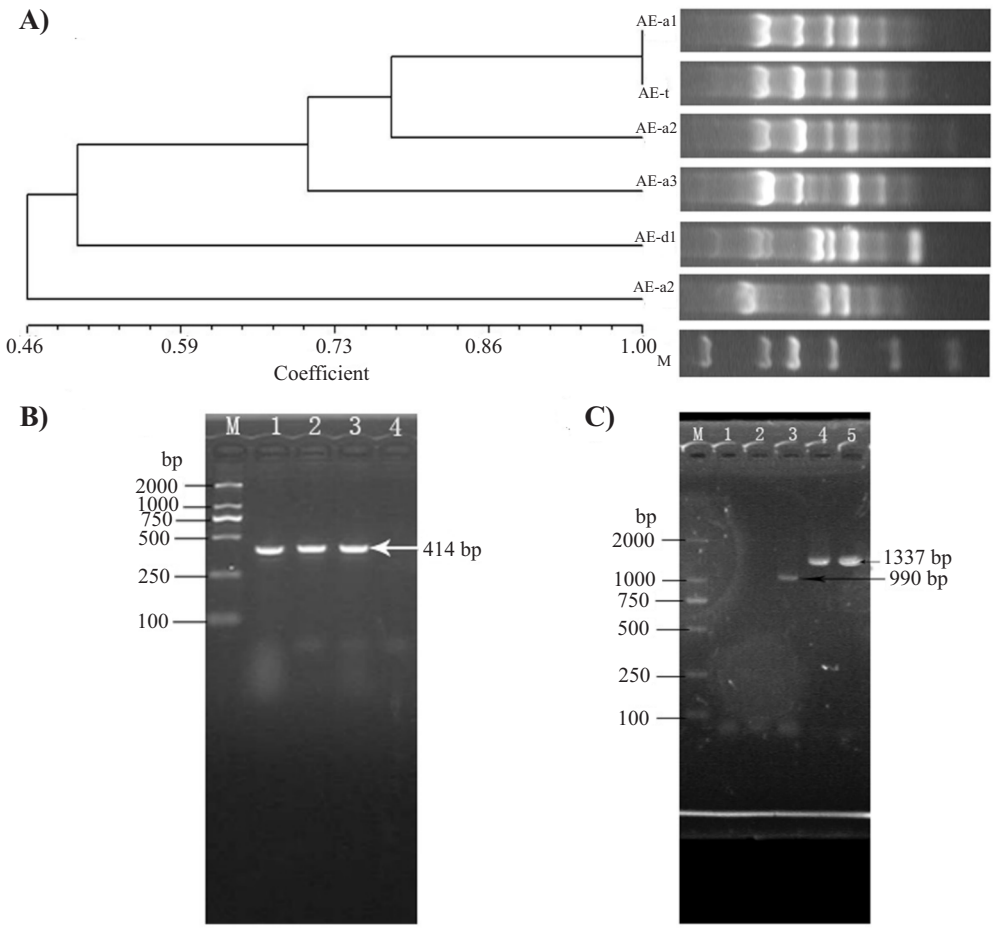

Fig. 1 ERIC-PCR and PCR results from the experimental stains. **A)** Dendrogram of ERIC-PCR results from the HPI$^+$ (positive) and HPI$^-$ (negative) *E. coli* isolates. The two HPI$^+$ wild *E. coli* strains (AE-d1and AE-d2), the three HPI$^-$ wild *E. coli* strains (AE-a1, AE-a2 and AE-a3) and a HPI$^+$ acceptor strains (AE-t) were inoculated and then their bacterial DNA was extracted and analyzed by ERIC-PCR. **B)** PCR amplification of the AE-a1, AE-d1, AE-d2 and AE-t *E. coli* stains' *irp2* gene. The two HPI$^+$ wild *E. coli* strains (AE-d1 and AE-d2), the HPI$^-$ wild *E. coli* strains (AE-a1, AE-a2 and AE-a3) and the HPI$^+$ acceptor strains (AE-t) were inoculated and then their bacterial DNA was extracted and amplificated of the four stains' *irp2* gene by PCR. Lane M denoted DL2000 DNA Marker. Lane 1 denoted *irp2* gene PCR product from the AE-d1 (positive reslut). Lane 2 denoted *irp2* gene PCR product from the AE-d2 (positive reslut). Lane 3 denoted *irp2* gene PCR product from the AE-t (positive reslut). Lane 4 denoted *irp2* gene PCR product from the AE-a1 (negative reslut). **C)** PCR amplification of the AE-a1, AE-d1, AE-d2 and AE-t *E. coli* stains' *intB* gene. The two HPI$^+$ wild *E. coli* strains (AE-d1 and AE-d2), the HPI$^-$ wild *E. coli* strains (AE-a1, AE-a2 and AE-a3) and the HPI$^+$ acceptor strains (AE-t) were inoculated and then their bacterial DNA was extracted and amplificated of the four stains' *intB* gene by PCR. Lane M denoted DL2000 DNA Marker. Lane 1 denoted *intB* gene PCR product from ddH_2O (negative reslut). Lane 2 denoted *intB* gene PCR product from the AE-a1 (negative reslut). Lane 3 denoted *intB* gene PCR product from the AE-d1 (positive reslut, product size=990bp). Lane 4 denoted *intB* gene PCR product from the AE-d2 (positive reslut, product size=13370bp). Lane 5 denoted *intB* gene PCR product from the AE-t (positive reslut, product size=1337bp).

was amplified by primers *irp2*-F/*irp2*-R from the AE-d1, AE-d2, and AE-t strains, while no product was amplified from the AE-a1 strain. In addition, a 1337-bp PCR product from the AE-t and AE-d2 strains, and a 990-bp PCR product from the AE-d1 strain were amplified by PCR using the *intB*-F/*intB*-R primers (Fig. 1C). The results confirmed that AE-t was the *HPI*$^+$ transfer strain, and that AE-d2 and AE-a1 was the donor and acceptor strain, respectively.

CAS siderophore detection assay

In this study, the AE-a1, AE-d2, and AE-t strains grew well on solid flat CAS plates (Fig. 2). After culturing for 2 d, transparent halos appeared around the colonies, and after 3 day, they reached their maximum diameters. However, the position of applied liquid LB in the negative control did not show a transparent halo on the solid plate. Based on the ratio of the diameter of the halo and the colony, it was determined

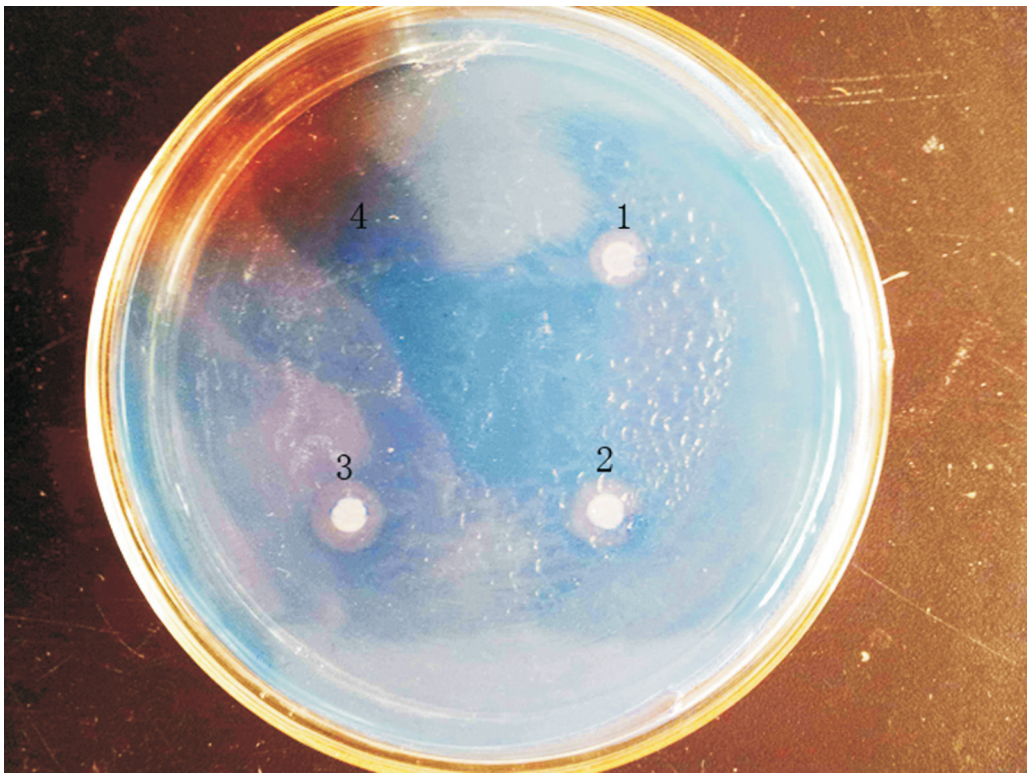

Fig. 2. Orange teliospores on CAS medium produced by the AE-a1, AE-d1 and AE-t *E. coli* stains. Inoculum 1 denoted AE-d1 stains. Inoculum 2 denoted AE-a1 stains. Inoculum 3 denoted AE-t strains. Inoculum 4 denoted LB medium as the control group.

Table 2. Siderophore-producing bacteria and the size of their halos.

Strain no.	Colony size (mm)	Halo size (mm)	The ratio of the diameter of the halo and colony
AE-d1	3.9	7	1.795
AE-a1	4	8.1	2.025
AE-t	4	8.9	2.225
Control	0	0	

that the experimental strains produced siderophores (Table 2).

Low iron stress test

The bacterial densities of the AE-a1 and AE-t strains under exposure to different concentrations of iron chelator 2,2'-bipyridine for 0-36 h incubation time are shown in Fig. 3. In culture medium without 2,2'-bipyridine, the AE-a1 strain grew better than the AE-t strain. When the 2,2'-bipyridine concentration was 0.128 mM, AE-a1 and AE-t was slightly inhibited. When the 2,2'-bipyridine concentration was greater than or equal to 0.256 mM, the growth of the two strains was significantly inhibited for 0-36 h. Thus, the inhibition of bacterial growth by 2,2'-bipyridine was concentration-dependent.

As incubation time at 0-36h increased, the abundance of the two strains increased. Within the first 12 h, the AE-t strain grew relatively rapidly. When the 2,2'-bipyridine concentration was less than 0.768 mM, the growth rates in the AE-a1 and AE-t strains were not significantly different. Therefore, *HPI* did not play a significant role in promoting the growth of bacteria in the first 12 h with exposure to a low concentration of iron chelator. However, after 24 h and before 36 h of culture at concentrations of 2,2'-bipyridine greater than or equal 0.256 mM, the quantity of bacteria was significantly different between the two strains, which showed that the *HPI* had a significant role in promoting the growth of bacteria after 12-24 h in low iron conditions. After 36 h of incubation or when the 2,2'-bipyridine concentration was greater than or equal 0.512 mM, the quantity of bacteria was not significantly different between the AE-a1 and AE-t strains.

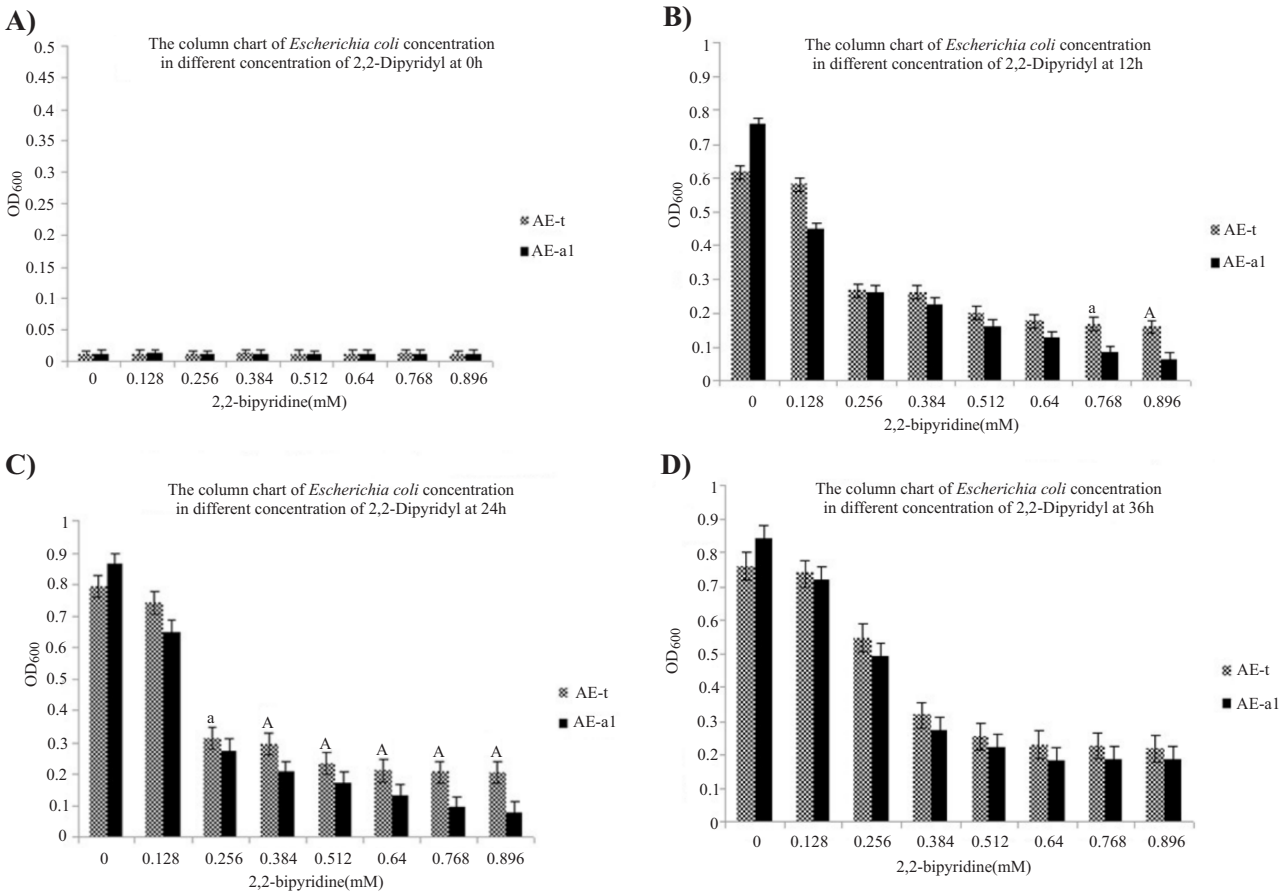

Fig. 3. AE-t and AE-a1 cellular abundance at different concentrations of 2,2'-bipyridine for 0-36 h incubation time. (A) AE-t and AE-a1 cellular abundance at different concentrations of 2,2'-bipyridine at 0 h. (B) AE-t and AE-a1 cellular abundance at different concentrations of 2,2'-bipyridine at 12 h. (C) AE-t and AE-a1 cellular abundance at different concentrations of 2,2'-bipyridine at 24 h. (D) AE-t and AE-a1 cellular abundance at different concentrations of 2,2'-bipyridine at 36 h. Data are expressed as mean ± SEM (n=3) and the columns designated by the upper-case letter *aA* are significantly different (*a*, $p<0.05$) and those designated by a lower-case *Aa* are very significantly different (*A*, $p<0.01$).

Bacterial adherence and invasion to DF-1 cells

Differences in adherence and invasion between the AE-t and AE-a1 groups were statistically significant ($p<0.01$). In addition, compared with the AE-a1 strain, the AE-t strain showed lower adherence and invasion to DF-1 cells, which were far different (Fig. 4).

Animal infection

After intraperitoneal inoculated (IP inoculation) with the bacteria, both groups of chicks showed significant symptom of depressed and diarrhea. The symptoms of the AE-a1-treated group were most severe with a mortality rate of 40% with clinical manifestations including air sacculitis, perihepatitis, pericarditis, peritonitis and salpingitis. However, the symptoms of the AE-t-treated group were mild with a mortality rate of 0 without clinical manifestations and this group returned to normal after 24 h. While some subjects died in the AE-a1 group, and AE-t group showed no pathogenicity, and no subjects in the control group died (Table 3). The dead chicks were necropsied, and those that died within 48 h of treatment had no obvious lesions, whereas the lesions of the chicks that died more than 48 h after treatment were primarily perihepatitis, air sac inflammation, and peritonitis.

Discussion

In the present study, all *HPI*s were located adjacent to the gene coding for Asn-tRNA, and in most bacteria the presence of P4 bacteriophages' integration sites. It suggests that Asn-tRNA plays a role in targeting gene transfer via bacteriophages and plasmids (Hacker and Kaper 2000), and thus that Asn-tRNA is a key element required for bacterial evolution. Lesic and Carniel (2005) discovered that

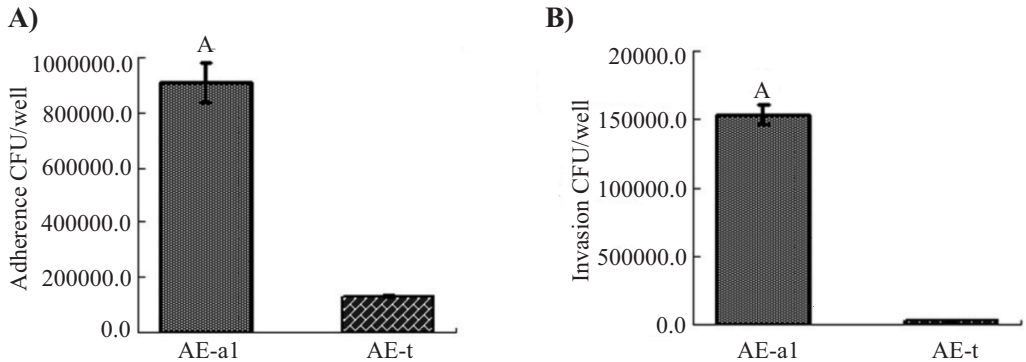

Fig. 4. Adhesion and invasion of AE-t and AE-a1 to DF-1 cells. (A) Adhesion of AE-a1 (the HPI- wild *E.coli* strains) and AE-t (the HPI+ acceptor strains strains) to DF-1 cells. (B) Invasion of AE-a1 and AE-t into DF-1 cells. The bacteria were counted and the invasion frequency was determined. Data are expressed as mean ± SEM (n=3) and the columns designated by the upper-case letter *A* are highly significantly different (*A*, $p<0.01$).

Table 3. Mortality of *E. coli*-infected chicks.

Group	Number of experimental animals	Number of dead animals	Mortality rate (%)
AE-a1	20	8	40
AE-t	20	0	0
Control	20	0	0

HPI transfer was dependent on homologous recombination in the recipient strain, and that adjacent contiguous sequences were also moved. The results of Asn-tRNA loci PCR amplification showed that restructuring also occurred outside the *HPI*. Lesic and Carniel (2005) also found that *HPI* had high transfer frequencies at low temperatures and in conditions of low iron abundance, which showed that bacteria were under selective pressure to acquire the complete *HPI.* After the *HPI* is obtained by host bacteria, survival in different environments may require adaptive change, in which the function of the *HPI* is deactivated. The complex process of horizontal transfer may offer an explanation for this process, which can abolish the expression of *HPI* genes. Lesic and Carniel (2005) also found that the growth of the *HPI* recipient strain was inhibited under normal conditions, and virulence was also significantly reduced. Probably due to the process of *HPI* transfer, homologous recombination in recipient strains leads to the deletion and destruction of growth and virulence genes.

The *HPI* of *Yersinia* encodes endogenous siderophores such as *Ybt,* and the functional inactivation of *Ybt* decreases virulence in mice. Several diverse iron uptake systems exist in bacteria, such as the aerobactin system, the enterobactin system, and the *PrrA-medD-yc73-fepC* system of urinary pathogenic *E. coli* (Guyer et al 1998).

The siderophores secreted from bacteria can chelate the $Fe3^{+}$ in CAS dye, which results in a color change from blue to orange, and thus an orange circle of siderophores will form on the CAS plate. Larger halo diameters under identical conditions indicate greater bacterial siderophore productive capacity. We found that the halo diameter of AE-t cells was larger than that of AE-a1 cells, but this difference was not significant. Therefore, further studies should determine whether *HPI*s promote iron uptake in avian *E. coli*.

In addition, we found that the growth rate of the AE-t strain was higher than that of the AE-a1 strain when the concentration of iron chelator in the growth medium was greater than or equal to 0.128 mM, and differences were greater during the first 24 h of exposure, suggesting that the adaptability of the AE-a1 strain under conditions of low iron abundance was strengthened by the *HPI*. Perhaps due to a strengthened ability to absorb iron, the abundance of each strain was not significantly different during the 24-36 h culture period. During this period, the AE-a1 strain grew slowly, demonstrating the iron intake ability of *HPI- E. coli*. However, the number of AE-t cells was almost unchanged, perhaps because the iron in the AE-t culture medium had been completely chelated, and the concentration was too low to be transported by the iron uptake system of the bacteria. Currently, knowledge of the function of *E. coli HPI*s is based on knowledge of the *Yersinia Ybt* iron uptake system. However, the influence of the efficient iron uptake system of *E. coli* may mask the contribution of the *HPI* to iron uptake. Therefore, we suggest that *HPI*s promote the growth of *E. coli* under condi-

tions of iron deficiency, likely via expression of siderophore *Ybt*, which functions in iron uptake.

While the *HPI* is thought to encode the *Ybt* siderophore, in general, changes in iron uptake in bacteria indirectly increase pathogenicity by enhancing metabolic adaptation, but do not directly result in infection or damage to the host (Miles and Khimji 1975, Hartmann and Braun 1981, Perry 1993, Zhou 1999). *HPI*s in *Yersinia* are not limited to pathogenic bacteria, and have also been detected in some conditionally pathogenic bacteria and non-pathogenic bacteria. Schubert (1998, 1999) has reported that 32% of *E. coli* isolated from healthy human feces have the *irp2*/*fyuA* cluster. Furthermore, only subtle differences in pathogenicity were found between *HPI*-positive and-negative strains of Shiga toxin-producing *E. coli* (STEC) (Karch et al. 1999). These results suggest that the *HPI* does not always confer pathogenicity. Indeed, the results of bacterial adherence and invasion and animal infection experiments showed that the pathogenicity of the *HPI* transfer strain was significantly less than that of the acceptor strain. Therefore, the *HPI* alone does not determine the pathogenicity of *E. coli*, but does so in combination with other virulence factors. The pathogenicity of *E. coli* is a comprehensive reflection of its production and reproductive performance and the effects of virulence genes. Here, we have shown that the *E. coli HPI* is a gene cluster that encodes products with iron uptake and virulence functions, but its main functions in pathogenic *E. coli* are not well understood and in need of further study.

Acknowledgments

This work was supported by funds from the National Natural Science Foundation of China (31502038), from the National Natural Science Foundation of China (31372402) and from the Natural Science Foundation of Anhui province (1508085SQC206).

References

Cheng D, Sun H, Xu J, Gao S (**2006**) PCR detection of virulence factor genes in *Escherichia coli* isolates from weaned piglets with edema disease and/or diarrhea in China. Veterinary Microbiology 115(4): 320-328.

Dho-Moulin M, Fairbrother JM (**1999**) Avian pathogenic *Escherichia coli* (APEC). Veterinary research. 30: 299-316.

Guyer DM, Kao JS, Mobley HL (**1998**) Genomic analysis of a pathogenicity island in uropathogenic escherichia coli cft073: distribution of homologous sequences among isolates from patients with pyelonephritis, cystitis, and catheter-associated bacteriuria and from fecal samples. Infection and Immunity 66(9): 4411-7.

Hacker J, Blum-Oehler G, Muhldorfer I, Tschape H (**1997**) Pathogenicity islands of virulent bacteria: structure, function and impact on microbial evolution. Mol Microbiol 23: 1089-1097.

Hacker J, Kaper J B (**2000**) Pathogenicity islands and the evolution of microbes. Annual Rev Microbiol 54: 641-679.

Heesemann J, Hantke K, Vocke T, Saken E, Rakin A, Stojiljkovic I, Berner R (**1993**) Virulence of Yersinia enterocolitica is closely associated with siderophore production, expression of an iron-repressible outer membrane polypeptide of 65,000 Da and pesticin sensitivity. Mol Microbiol 8: 397-408.

Hartmann A, Braun V (1**981**) Iron uptake and iron limited growth of *Escherichia coli* K-12. Arch Microbiol 130: 353-356.

Kaper JB, Nataro JP, Mobley HL (**2004**) Pathogenic escherichia coli. Nature Reviews Microbiology, 2(2): 123-40.

Karch H, Schubert S, Zhang D, Zhang W, Schmidt H, Olschlager T, Hacker J (**1999**) A genomic island, termed high-pathogenicity island, is present in certain non-O157 Shiga toxin-producing Escherichia coli clonal lineages. Infect Immun 67: 5994-6001.

Lesic B, Carniel E (**2005**) Horizontal transfer of the high-pathogenicity island of Yersinia pseudotuberculosis. J Bacteriol 187: 3352-3358.

Miles AA, Khimji PL (**1975**) Enterobacterial chelators of iron: their occurrence, detection, and relation to pathogenicity. J Med Microbiol 8: 477-490.

Pelludat C, Rakin A, Jacobi C A, Schubert S, Heesemann J (**1998**) The yersiniabactin biosynthetic gene cluster of Yersinia enterocolitica: organization and siderophore-dependent regulation. J Bacteriol 180: 538-546.

Perry RD (**1993**) Acquisition and storage of inorganic iron and hemin by the yersiniae. Trends Microbiol 1: 142-147.

Rakin A, Noelting C, Schubert S, Heesemann J (**1999**) Common and specific characteristics of the high-pathogenicity island of yersinia enterocolitica. Infection and Immunity 67(10): 5265-74.

Schubert S, Rakin A, Fischer D, Sorsa J, Heesemann J (**1999**) Characterization of the integration site of yersinia high-pathogenicity island in escherichia coli. Fems Microbiology Letters 179(2): 409.

Schubert S, Rakin A, Karch H, Carniel E, Heesemann J (**1998**) Prevalence of the "high-pathogenicity island" of Yersinia species among Escherichia coli strains that are pathogenic to humans. Infect Immun 66: 480-485.

Schwyn B, Neilands JB (**1987**) Universal chemical assay for the detection and determination of siderophores. Anal Biochem 160: 47-56.

Versalovic J, Koeuth T, Lupski JR (**1991**) Distribution of repetitive DNA sequences in eubacteria and application to fingerprinting of bacterial genomes. Nucleic Acids Res 19: 6823-6831.

Xu L, Qi K, Peng K (**2010**) Detection of the core area located on yersinia high pathogenicity island in the avian pathogenic escherichia coli strain(CVCC1565). Journal of Biology 27(6): 49-50.

Zhou D, Hardt WD, Galan JE (**1999**) Salmonella typhimurium encodes a putative iron transport system within the centisome 63 pathogenicity island. Infect Immun 67: 1974-1981.